

Online Monitoring of Object Detection Performance Post-Deployment

Quazi Marufur Rahman, Niko Sünderhauf and Feras Dayoub

Abstract— Post-deployment, an object detector is expected to operate at a similar level of performance that was reported on its testing dataset. However, when deployed onboard mobile robots that operate under varying and complex environmental conditions, the detector’s performance can fluctuate and occasionally degrade severely without warning. Undetected, this can lead the robot to take unsafe and risky actions based on low-quality and unreliable object detections. We address this problem and introduce a cascaded neural network that monitors the performance of the object detector by predicting the quality of its mean average precision (mAP) on a sliding window of the input frames. The proposed cascaded network exploits the internal features from the deep neural network of the object detector. We evaluate our proposed approach using different combinations of autonomous driving datasets and object detectors.

I. INTRODUCTION

Object detection plays a vital role in many robotics and autonomous system applications. For instance, a driver-less car is expected to detect important objects such as vehicles, people and traffic signs accurately all the time. Failure to do so can cause severe consequences for the car and the people involved. Hence, there is ongoing research [1]–[10] to improve the robustness and accuracy of object detection systems. In general, an object detection system is trained and evaluated using non-overlapping training, validation, and test splits of a dataset before deployment. The underlying assumption is that the images encountered during deployment follow a similar distribution to the images presented before deployment. However, in the case of autonomous systems, the post-deployment environment can exhibit many conditions that are not well represented in the pre-deployment datasets. This leads to the fact that post-deployment performance can fluctuate and may diverge from the expected pre-deployment performance without any prior warning. Such silent change in the post-deployment performance is a serious concern for any vision-based robotic system, see Fig. 1.

The ultimate solution to meet this challenge is to develop a remarkably persistent object detection system by collecting training data from all imaginable conditions that can be encountered post-deployment. As such a solution is not practical, one remedy to this situation is to deploy a performance monitoring system for the object detector that can raise warnings when the performance drops below a critical threshold.

The authors are with the Australian Centre for Robotic Vision at Queensland University of Technology (QUT), Brisbane, QLD 4001, Australia. This research has been conducted by the Australian Research Council (ARC) Centre of Excellence for Robotic Vision (Grant CE140100016). The authors acknowledge continued support from the QUT Centre for Robotics. Contact: quazi.rahman@qut.edu.au

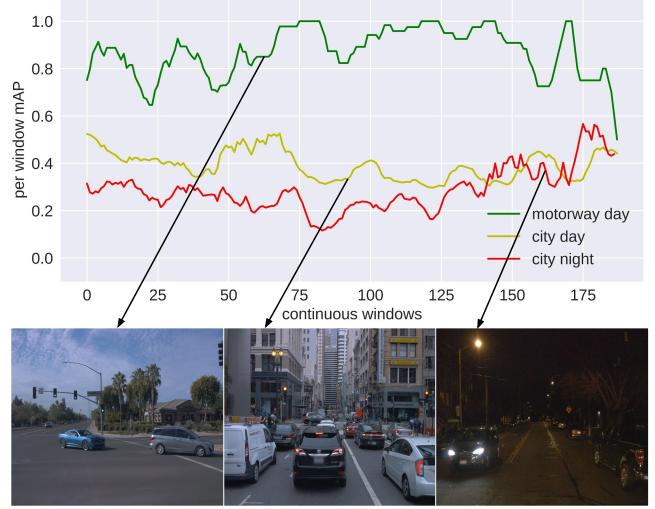


Fig. 1: The performance of an object detector deployed on a self-driving car depends heavily on the environmental conditions, such as traffic density, road type, and time of day. The mAP (calculated over a sliding window of 10 frames) even fluctuates significantly within each scenario. We show that a specialised performance monitoring network can predict the mAP of the object detector to inform downstream tasks of its expected reliability. In this figure, the first row shows the fluctuating mAP of three road scenes (motorway day, city day and night). The second row shows one sample image from each road scene.

A performance monitoring system is expected to provide the capability of self-assessment to the object detector. This self-assessment can improve safety and robustness post-deployment by monitoring the performance continuously and allowing to take preventive measures when the performance seems lower than expected.

To this end, the contribution of this paper is a novel cascaded neural network that exploits the internal feature maps from the deep neural network of the object detector for the task of online performance monitoring. Our proposed cascaded network operates on a sliding window of frames and continuously predicts the performance of the object detector in terms of mean average precision (mAP). We evaluate our proposed approach against multiple baselines using different combinations of datasets and object detection networks.

The rest of the paper is organized as follows: In Section II, we review the related works on performance monitoring. In Section III, we introduce our method for online performance

monitoring of object detection post-deployment. Section IV outlines our experimental setup. Section V presents the results and finally in Section VI we draw conclusion for this work.

II. RELATED WORKS

Self-assessment and performance monitoring in robotics applications is an important capability due to the high requirements of safety and robustness. In [11], a framework called robotic introspection is developed to provide self-assessment mechanism for field robots during exploration and mapping of subterranean environments. Later [12] and [13] extended this work for obstacle avoidance and semantic mapping assessment. These works examine the output of the underlying models to predict their expected performance.

Another approach to address the performance monitoring problem is to evaluate model input before inference. [14] proposed a framework following this paradigm. They train an alert module to find cases where the target model will fail. Later, a similar approach was used for failure prediction for MAV [15], hardness predictor [16] for image classifiers and probabilistic performance monitoring for robot perception system [17] for the task of pedestrian detection based on past experience from repeated visits to the same location.

Exploiting model confidence and uncertainty is another line of research to monitor the performance of a target model. Trust score [18], maximum class probability [19] and true class probability [20] are some recent works based on model confidence to identify the failure of an underlying image classifier. In the context of uncertainty estimation, [21] proposed to use dropout as a Bayesian approximation technique to represent model uncertainty. Later, [22], [23] applied this idea to identify the quality of image and video segmentation network.

In the object detection context, there are few works which address the performance monitoring to some extent. [24] and [25] use dropout sampling and hard false positive mining respectively to identify object detection failures. [26] and [27] use internal and hand-crafted features of an object detector respectively to identify false negative instances during deployment. These works focus on a per-object and per-frame basis and do not provide an overall assessment of the object detector performance considering the combined aspects of false positives, false negatives and object localization accuracy. These aspects are captured by a summary metric such as mAP. Our proposed approach can monitor object detection performance online by predicting the quality of its mAP for a sequence of images during the deployment phase without using any ground-truth data.

III. APPROACH OVERVIEW

In this section, we present our approach to online monitoring of object detection performance during the deployment phase. We start by formalizing the problem, and then we describe our proposed cascaded neural network architecture

that operates on the feature stream generated by the underlying object detection network to monitor its performance in real-time.

Let us denote an object detection network as od_{net} that is mounted on a driver-less car to detect object of interest like vehicle and pedestrian from the road. It takes a continuous stream of images $I = \{I_1, I_2, \dots, I_N\}$ and detect all possible objects from each I_i . Our goal is to monitor the performance of od_{net} by predicting its mAP continuously over a sliding window of images.

As described by [28], modern deep CNN's become unstable when the input image is translated, rescaled or slightly transformed by any other means. This observation holds for object detector deployed on a driver-less car too, where the mAP between two consecutive frames might vary significantly because of irrelevant or negligible changes in the viewpoint. As a result, per-frame performance monitoring can raise unnecessary false alarms. To mitigate this issue, we are adopting per sliding window performance monitoring, where the mAP between two consecutive windows does not change drastically. Hence, the performance monitoring network is expected to produce a consistent prediction by examining a sequence of images. To achieve this, we will deploy a second convolutional neural network that will access the internal features of od_{net} to predict the quality of the mAP for each sliding window of images. This second network will be referred as performance monitoring network, pm_{net} .

Instead of processing each input image I_i like od_{net} does at a time, pm_{net} operates on ω sequential images and predict the overall mAP of od_{net} on these ω images. We will use ω to refer the window size used by pm_{net} . Here, pm_{net} takes a stream of windows $W = \{W_1, W_2, \dots, W_M\}$ and monitor the performance for each W_i , where $W_i = \{I_i, I_{i+1}, \dots, I_{i+\omega}\}$.

We formulate the task of performance monitoring as a multi-class classification problem consisting of C classes. To do so, the per-window mAP range is split into C equal and consecutive parts and labeled from 0 to $C-1$. We will denote these per-window mAP label using mAP_w . The lowest and the highest label, 0 and $C-1$ refer to the worst and the best possible classes respectively. As there is an ordinal relation among these labels, we will consider this multi-class classification problem as ordinal classification [29].

Our proposed pm_{net} exploits the features generated by od_{net} during per frame inference. od_{net} uses a backbone architecture B to extract features for the inference task where B is a collection of interconnected convolutional layers. During the inference, for each image I_i , B generates a set of p feature maps, $L_i = \{L_{i1}, L_{i2}, \dots, L_{ip}\}$. Here, shape of L_{ij} is $c_{ij} \times h_{ij} \times w_{ij}$. c_{ij} , w_{ij} and h_{ij} are the channel, width and height of the j^{th} convolutional layer of the i^{th} image.

After each inference pm_{net} extracts L_i from B for input I_i and apply channel-wise average pooling to convert each $3D$ features into $2D$. Now the converted set of feature is $\bar{L}_i = \{\bar{L}_{i1}, \bar{L}_{i2}, \dots, \bar{L}_{ip}\}$ and shape of \bar{L}_{ij} is $1 \times h_{ij} \times w_{ij}$. This operations are performed for all I_i and the newly formed

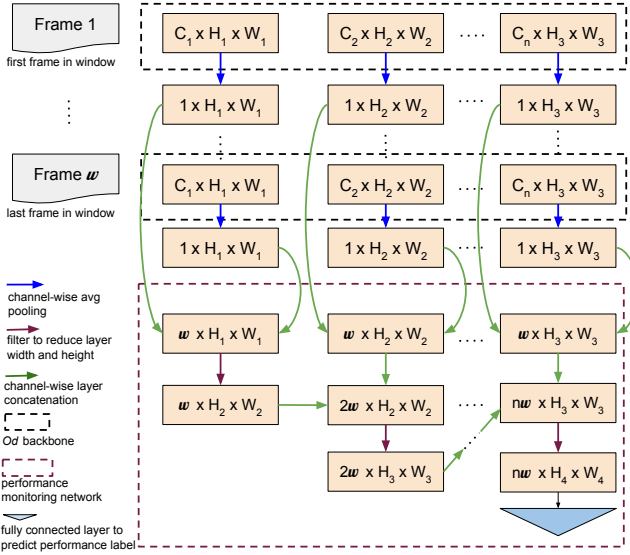


Fig. 2: Cascaded architecture of the proposed performance monitoring network. First four rows show the procedure to convert 3D feature from frame 1 to ω into 2D. These features are collected from the object detection backbone. 5th row demonstrates how the 2D features from corresponding layers are stacked together to generate a ω channel 3D feature. 6th and 7th rows represent how each feature is cascaded with the previous one.

corresponding 2D features are stacked together in channel-wise direction. That means the $\bar{L}_{(i+1)j}$ is stacked with \bar{L}_{ij} . After processing ω images we get feature F_{W_i} for W_i . Here $F_{W_i} = \{F_1, F_2, \dots, F_p\}$ and F_i has the size of $\omega \times h_{ij} \times w_{ij}$. The task of pm_{net} is to predict mAP_w from F_W .

We design the pm_{net} as a cascaded convolutional neural network to train it to predict mAP_w from F_W . Here, each layer of pm_{net} is implicitly connected with all the previous layers through their individual convolutional filter. Using this network, we exploit the rich multi-level semantic features generated by the od_{net} instead of only using the last convolutional layer features. pm_{net} uses a set of convolutional filter $f = \{f_1, f_2, \dots, f_{p-1}\}$ to propagate the features of F_W from one layer to the next. Each filter f_i operates on F_i to generate a new feature \bar{F}_i which has the same shape of F_{i+1} . Now a concatenation is performed to join \bar{F}_i and F_{i+1} in channel-wise direction. This set of operation can be formulated using Equation 1.

$$\mathcal{F} = f_i(F_i) \oplus F_{i+1}; \quad i = 1, 2, \dots, p-1 \quad (1)$$

Next, we apply adaptive average pooling operation on \mathcal{F} to generate a one dimensional feature vector. This features is passed through subsequent fully connected layers to generate the final prediction for F_W . See Fig. 2 for a visualisation of these procedures.

IV. EXPERIMENTAL SETUP

In this section we will describe the settings that we used to evaluate our proposed approach.

A. Experimental Steps

We can describe the overall experimental procedure using three steps. At first an object detector is trained using transfer learning technique to detect different objects (vehicle, pedestrian) from a dataset named as *primary training dataset*. In the next step, the detector is used to detect the similar objects from another dataset (*secondary training dataset*) which was not used during the initial training phase. This *secondary training dataset* consists of stream of images. In this step, a sequential stream of images is fed to the object detector and for each consecutive window of images we collect the features for each window and calculate the corresponding mAP using the *secondary training dataset* as groundtruth. Then, we train the proposed cascaded CNN, pm_{net} to predict the mAP from the collected per-window features. Next, we use multiple metrics and another image stream dataset (*test dataset*) unused in previous steps to evaluate the proposed approach. See Fig. 3 for a high-level overview of these steps.

B. Dataset

We used multiple combination of three different datasets (KITTI [30], BDD [31], Waymo [32]) to conduct all the experiments. In each settings, one dataset from KITTI and BDD has been used as *primary training dataset*. Then we used one of the video datasets from KITTI, BDD and Waymo as the *secondary training dataset* which was not a part of *primary training dataset*. To evaluate the system we used one video dataset that was unused as *primary training dataset* or *secondary training dataset*.

C. Training

We trained two-stage Faster RCNN [2] and one-stage RetinaNet [33] object detection networks pre-trained on MS-COCO [34] dataset to detect vehicle and pedestrian from the KITTI and BDD dataset. Both of these networks use ResNet50 [35] as their backbone. To be interoperable among multiple datasets, classes like car, van, tram and bus have been assigned to vehicle class. Besides, pedestrian and person classes from all the datasets are denoted as pedestrian class. Moreover, objects less than 25 pixel in width or height are removed from all the datasets. To generalize the object detection and performance monitoring network training, we applied several weather related augmentation (random fog, snow and rain). Table I shows the object detection accuracy in mAP for *primary training dataset* and object detection network settings.

We adopted the CORAL [36] framework that uses a set of binary classifier to train pm_{net} as an ordinal classifier.

TABLE I: Object detection accuracy in mAP for FRCNN and RetinaNet network on KITTI and BDD100K dataset for detecting vehicle and pedestrian.

Model	KITTI	BDD
FRCNN	66.0%	52.4%
RetinaNet	60.58%	65.49%

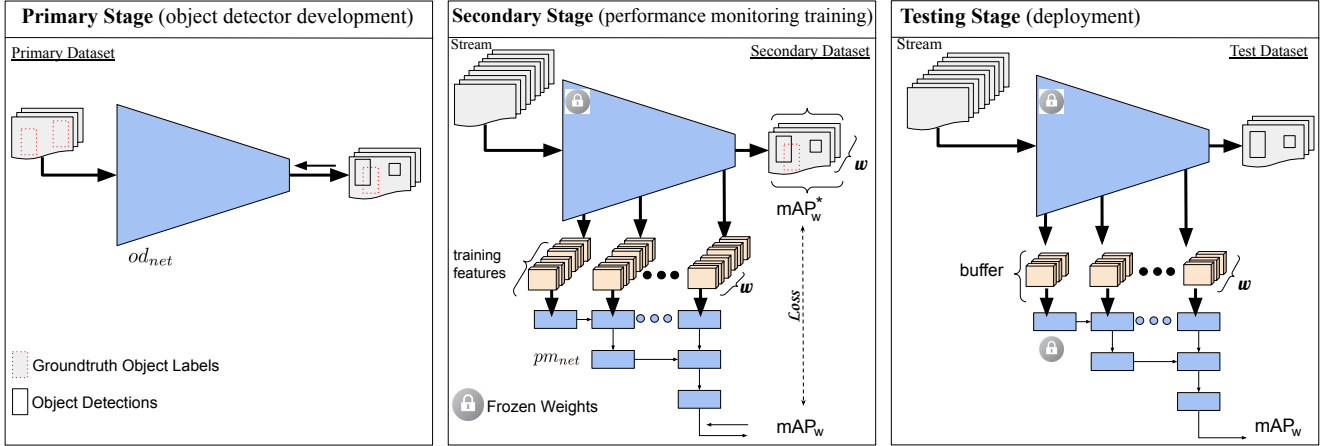


Fig. 3: An overview of the three stages for training and testing our performance monitoring network (pm_{net}). First, the object detector is developed using a *primary training dataset*. After the training is done, a *secondary training dataset* consisting of video streams is used to collect inner features from the backbone network of the object detector and train pm_{net} to predict the quality of the detector’s per-window mAP. Finally, a third *test dataset* of video streams is used to evaluate the performance monitoring network. The three datasets are independent of each other.

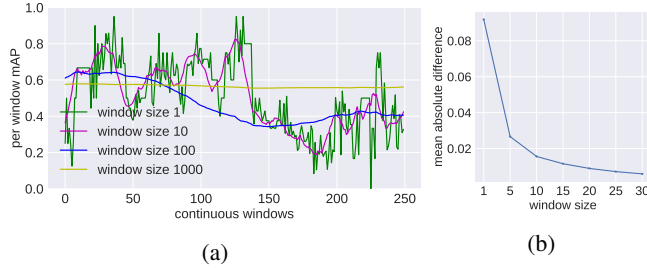


Fig. 4: (a) per-window mAP for multiple lengths of continuous windows. (b) mean absolute difference between two consecutive per-window mAP for different length of continuous windows.

Each binary classifier predicts whether per-window mAP is within a particular range. This prediction is controlled by a decision threshold. The ordinal classifier has 5 classes from 0 to 4 each incrementally spanning 0.2 per-window mAP. In this case, class 2 is equivalent per-window mAP below 0.4. To train the pm_{net} , we used the Adam optimizer [37] and a initial learning rate of 0.001 with batch size 32.

For all of the following experiments, we use a sliding window of 10 frames. We empirically found that this value provides a balance between the high sensitivity of smaller windows and the smoothing effect of large windows as shown in Fig. 4.

D. Evaluation Metrics

We used mean absolute error (MAE), root mean squared error (RMSE) and zero-one error (ZOE) [38], which is the fraction of incorrect classification, as the evaluation metric for pm_{net} ordinal classification task. To compare with the baselines and to evaluate how well the pm_{net} can detect critical mAP label we used true positive rate at 5% false positive rate (TPR@FPR5) , false positive rate at 95% true

positive rate (FPR@TPR95) and area under the ROC curve (AUROC) metric.

E. Baseline Approaches

Baseline 1: In [27], Ramanagopal et. al. proposed an approach to identify perception failure of an object detection system. They used manually selected features like bounding box confidence and their mean and median overlap to identify false negative instances generated by an object detector. Following their approach, in this baseline we extract a set of features from each image after performing the object detection. This set includes mean and median of all detected bounding box confidences, mean and median overlap, width and height of all detected bounding boxes in normalized scale. We extracted these features from all images of each window and concatenated them together to generate a one dimensional feature corresponding the window. Next, each mAP per-window is converted into a binary label using a critical threshold 0.4. Any mAP which is lower than this threshold is assigned to positive class otherwise negative. Next we train a fully connected binary classifier to predict the probability of each window to be assigned in the positive or negative class.

Baseline 2: In this baseline we are using internal features from the last convolutional layer of a trained object detector backbone instead of hand crafted features. After each inference, we collect the 3D features from the last backbone layer and apply the average pooling technique to convert that 3D features into 1D. After concatenating all 1D features from all images of a window, we get a feature corresponding to that window. Using the critical threshold discussed in baseline 1, we assign each window into positive and negative classes. Then a fully connected binary classifier is trained to predict these classes from the window feature.

We use class 2 which is equivalent to critical threshold 0.4

TABLE II: MAE, RMSE and ZOE score for pm_{net} trained using features collected from FRCNN backbone.

Primary	Datasets Secondary	Test	MAE	RMSE	ZOE
			bdd	kitti	waymo
bdd	waymo	kitti	0.181	0.428	0.180
kitti	bdd	waymo	0.302	0.569	0.346
kitti	waymo	bdd	0.241	0.496	0.269

TABLE III: MAE, RMSE and ZOE score for pm_{net} trained using features collected from RetinaNet backbone.

Primary	Datasets Secondary	Test	MAE	RMSE	ZOE
			bdd	kitti	waymo
bdd	waymo	kitti	0.272	0.523	0.259
kitti	bdd	waymo	0.275	0.554	0.266
kitti	waymo	bdd	0.290	0.561	0.277

to treat our ordinal classifier output as a binary classification. Consequently, classes from 0 to 1 and 2 to 4 are assigned to positive and negative classes respectively. This conversion allows to compare our ordinal classifier with the binary classifier based baselines.

V. EVALUATION AND RESULTS

In this section, firstly, we summarize how well the proposed performance monitoring network works as an ordinal classifier. Secondly, we evaluate the accuracy of the proposed network to detect when per-window mAP drops below the critical threshold of 0.4.

Experiment 1: Table II shows the pm_{net} ordinal classification accuracy using MAE, RMSE and ZOE error metric for four different dataset settings. Here, od_{net} is trained using FRCNN and pm_{net} is trained and evaluated using FRCNN backbone features. The second row shows pm_{net} error metric for ordinally classifying od_{net} performance on the KITTI *test dataset*. od_{net} and pm_{net} are trained using *primary training dataset* BDD and *secondary training dataset* Waymo respectively. This settings demonstrates the lowest error in all the dataset settings.

Table III presents pm_{net} error metric for similar dataset settings as Table II. Here, od_{net} is trained using RetinaNet object detection network and pm_{net} is trained and evaluated using RetinaNet backbone features. In this table, *primary training dataset* BDD, *secondary training dataset* Waymo and *test dataset* KITTI demonstrates the lowest error than other dataset settings. This observation is consistent with Table II and suggests that the large diversity of BDD and Waymo dataset are effective for the performance monitoring of pm_{net} in the KITTI dataset.

Experiment 2: This experiment compares the proposed performance monitoring network with the baselines.

During the pm_{net} evaluation, the decision threshold is varied from 0 to 1 to produce the 5 class ordinal prediction for each threshold. Then using the critical threshold the ordinal class prediction is converted to a binary prediction

TABLE IV: pm_{net} comparison with other baselines. pm_{net} is trained using features collected from FRCNN backbone.

Metric	Primary	Datasets Secondary	Test	Ours	Base- line 2	Base- line 1
				TPR@	0.882	0.270
FPR5↑	bdd	kitti	waymo	0.922	0.378	0.080
	kitti	bdd	waymo	0.916	0.320	0.157
	kitti	waymo	bdd	0.897	0.513	0.133
FPR@	bdd	kitti	waymo	0.064	0.775	0.707
TPR95↓	bdd	waymo	kitti	0.093	0.557	0.777
	kitti	bdd	waymo	0.133	0.766	0.827
	kitti	waymo	bdd	0.054	0.457	0.948
AUROC	bdd	kitti	waymo	0.873	0.644	0.648
↑	bdd	waymo	kitti	0.891	0.589	0.537
	kitti	bdd	waymo	0.892	0.610	0.573
	kitti	waymo	bdd	0.929	0.560	0.528

TABLE V: pm_{net} comparison with other baselines. pm_{net} is trained using features collected from RetinaNet backbone.

Metric	Primary	Datasets Secondary	Test	Ours	Base- line 2	Base- line 1
				TPR@	0.875	0.228
FPR5↑	bdd	kitti	waymo	0.953	0.380	0.080
	kitti	bdd	waymo	0.915	0.576	0.214
	kitti	waymo	bdd	0.889	0.708	0.133
FPR@	bdd	kitti	waymo	0.098	0.576	0.827
TPR95↓	bdd	waymo	kitti	0.109	0.765	0.777
	kitti	bdd	waymo	0.053	0.479	0.707
	kitti	waymo	bdd	0.076	0.911	0.948
AUROC	bdd	kitti	waymo	0.860	0.567	0.573
↑	bdd	waymo	kitti	0.917	0.596	0.537
	kitti	bdd	waymo	0.915	0.564	0.648
	kitti	waymo	bdd	0.873	0.746	0.528

to compute the TPR and FPR. Therefore, each decision threshold generates a pair of TPR, FPR and using these metrics we calculate the TPR@FPR5, FPR@TPR95 and AUROC for our proposed approach.

As the two baselines use binary classifier approach, we can use their predicted positive class probability and corresponding groundtruth to calculate the TPR@FPR5, FPR@TPR95 and AUROC metric.

Table IV shows the comparison between pm_{net} and the two baselines using multiple metrics. For this table, the od_{net} is trained using FRCNN and the pm_{net} is trained and evaluated using FRCNN backbone features. In terms of TPR@FPR5, pm_{net} outperforms both of the baselines by a large margin. While the maximum TPR@FPR5 for pm_{net} over four dataset settings is 0.922, baseline 1 and 2 reach at maximum 0.214 and 0.513 respectively. For FPR@TPR95 the minimum score for our proposed approach is 0.054. However, the minimum FPR@TPR95 for baseline 1 and 2 is 0.707 and 0.457 respectively. In AUROC metrics, pm_{net} performs better than the baselines by obtaining 0.929 while the maximum AUROC of both baselines is 0.610. Although we have referred only the maximum score of each individual metrics from the four dataset settings, our proposed approach outperforms the baselines in all metrics and dataset settings.

Table V represents the comparative accuracy among pm_{net} and two other baselines. Here, the underlying object detector is trained using RetinaNet network and the corresponding performance monitoring network is trained and evaluated using features collected from RetinaNet backbone. In this case, for TPR@FPR5 metric, the maximum score that our proposed approach achieves out of four dataset settings is 0.953 while the maximum of two baselines among this four settings is 0.708. In case of FPT@TPR95 and AUROC, our proposed approach outperforms both of the baselines by a large margin.

Experiment 3: In order to monitor object detection performance online we are required to simultaneously use the performance monitoring network along with the object detection system. Hence, the inference time and GPU memory requirement of pm_{net} should be minimal for practical usage. On average pm_{net} and od_{net} inference time is 3.34 ± 0.126 ms and 28.11 ± 0.404 ms in our TITAN V GPU workstation. Besides, pm_{net} uses 243 MB of GPU memory which is 20.81% of memory used by the od_{net} .

VI. CONCLUSION

As deep learning-based object detection become essential components of a wide variety of robotic systems, the ability to continuously assess and monitor their performance during the deployment phase become critical to ensure the safety and reliability of the whole system. In this paper, we proposed a specialised performance monitoring network that can predict the quality of the mAP of the object detector, which can be used to inform downstream components in the robotic system about the expected object detection reliability. We show the effectiveness of our approach using a combination of different autonomous driving datasets and object detectors.

REFERENCES

- [1] Z. Tian, C. Shen, H. Chen, and T. He, “Fcos: Fully convolutional one-stage object detection,” in *Proceedings of the IEEE international conference on computer vision*, 2019, pp. 9627–9636.
- [2] S. Ren, K. He, R. Girshick, and J. Sun, “Faster r-cnn: Towards real-time object detection with region proposal networks,” in *Advances in neural information processing systems*, 2015, pp. 91–99.
- [3] W. Liu, D. Anguelov, D. Erhan, C. Szegedy, S. Reed, C.-Y. Fu, and A. C. Berg, “Ssd: Single shot multibox detector,” in *European conference on computer vision*. Springer, 2016, pp. 21–37.
- [4] K. Duan, S. Bai, L. Xie, H. Qi, Q. Huang, and Q. Tian, “Centernet: Keypoint triplets for object detection,” 2019 *IEEE/CVF International Conference on Computer Vision (ICCV)*, pp. 6568–6577, 2019.
- [5] A. Bochkovskiy, C.-Y. Wang, and H.-Y. M. Liao, “Yolov4: Optimal speed and accuracy of object detection,” *ArXiv*, vol. abs/2004.10934, 2020.
- [6] K. He, R. B. Girshick, and P. Dollár, “Rethinking imagenet pre-training,” 2019 *IEEE/CVF International Conference on Computer Vision (ICCV)*, pp. 4917–4926, 2019.
- [7] Z. Cai and N. Vasconcelos, “Cascade r-cnn: Delving into high quality object detection,” 2018 *IEEE/CVF Conference on Computer Vision and Pattern Recognition*, pp. 6154–6162, 2018.
- [8] Z. Li, C. Peng, G. Yu, X. Zhang, Y. Deng, and J. Sun, “Detnet: A backbone network for object detection,” *ArXiv*, vol. abs/1804.06215, 2018.
- [9] T.-Y. Lin, P. Goyal, R. B. Girshick, K. He, and P. Dollár, “Focal loss for dense object detection,” 2017 *IEEE International Conference on Computer Vision (ICCV)*, pp. 2999–3007, 2017.
- [10] N. Carion, F. Massa, G. Synnaeve, N. Usunier, A. M. Kirillov, and S. Zagoruyko, “End-to-end object detection with transformers,” *ArXiv*, vol. abs/2005.12872, 2020.
- [11] A. C. Morris, “Robotic introspection for exploration and mapping of subterranean environments,” Ph.D. dissertation, Carnegie Mellon University, The Robotics Institute, 2007.
- [12] H. Grimmett, R. Triebel, R. Paul, and I. Posner, “Introspective classification for robot perception,” *The International Journal of Robotics Research*, vol. 35, no. 7, pp. 743–762, 2016.
- [13] R. Triebel, H. Grimmett, R. Paul, and I. Posner, “Driven learning for driving: How introspection improves semantic mapping,” in *ISRR*, 2013.
- [14] P. Zhang, J. Wang, A. Farhadi, M. Hebert, and D. Parikh, “Predicting failures of vision systems,” in *Proceedings of the IEEE Conference on Computer Vision and Pattern Recognition*, 2014, pp. 3566–3573.
- [15] S. Daftry, S. Zeng, J. A. Bagnell, and M. Hebert, “Introspective perception: Learning to predict failures in vision systems,” in *2016 IEEE/RSJ International Conference on Intelligent Robots and Systems (IROS)*. IEEE, 2016, pp. 1743–1750.
- [16] P. Wang and N. Vasconcelos, “Towards realistic predictors,” in *Proceedings of the European Conference on Computer Vision (ECCV)*, 2018, pp. 36–51.
- [17] C. Gurau, D. Rao, C. H. Tong, and I. Posner, “Learn from experience: Probabilistic prediction of perception performance to avoid failure,” *The International Journal of Robotics Research*, vol. 37, pp. 981 – 995, 2018.
- [18] H. Jiang, B. Kim, and M. R. Gupta, “To trust or not to trust a classifier,” in *NeurIPS*, 2018.
- [19] D. Hendrycks and K. Gimpel, “A baseline for detecting misclassified and out-of-distribution examples in neural networks,” *ArXiv*, vol. abs/1610.02136, 2017.
- [20] C. Corbière, N. Thome, A. Bar-Hen, M. Cord, and P. Pérez, “Addressing failure prediction by learning model confidence,” in *Advances in Neural Information Processing Systems*, 2019, pp. 2902–2913.
- [21] Y. Gal and Z. Ghahramani, “Dropout as a bayesian approximation: Representing model uncertainty in deep learning,” in *ICML*, 2016.
- [22] T. Devries and G. W. Taylor, “Leveraging uncertainty estimates for predicting segmentation quality,” *ArXiv*, vol. 1807.00502, 2018.
- [23] P.-Y. Huang, W. T. Hsu, C.-Y. Chiu, T.-F. Wu, and M. Sun, “Efficient uncertainty estimation for semantic segmentation in videos,” in *ECCV*, 2018.
- [24] D. Miller, L. Nicholson, F. Dayoub, and N. Sünderhauf, “Dropout sampling for robust object detection in open-set conditions,” 2018 *IEEE International Conference on Robotics and Automation (ICRA)*, pp. 1–7, 2018.
- [25] B. Cheng, Y. Wei, H. Shi, R. S. Feris, J. Xiong, and T. S. Huang, “Decoupled classification refinement: Hard false positive suppression for object detection,” *ArXiv*, vol. abs/1810.04002, 2018.
- [26] Q. M. Rahman, N. Sünderhauf, and F. Dayoub, “Did you miss the sign? a false negative alarm system for traffic sign detectors,” 2019 *IEEE/RSJ International Conference on Intelligent Robots and Systems (IROS)*, pp. 3748–3753, 2019.
- [27] M. S. Ramanagopal, C. Anderson, R. Vasudevan, and M. Johnson-Roberson, “Failing to learn: Autonomously identifying perception failures for self-driving cars,” *IEEE Robotics and Automation Letters*, vol. 3, pp. 3860–3867, 2018.
- [28] A. Azulay and Y. Weiss, “Why do deep convolutional networks generalize so poorly to small image transformations?” *arXiv preprint arXiv:1805.12177*, 2018.
- [29] J. S. Cardoso and J. F. Costa, “Learning to classify ordinal data: The data replication method,” *Journal of Machine Learning Research*, vol. 8, no. Jul, pp. 1393–1429, 2007.
- [30] A. Geiger, P. Lenz, and R. Urtasun, “Are we ready for autonomous driving? the kitti vision benchmark suite,” in *Conference on Computer Vision and Pattern Recognition (CVPR)*, 2012.
- [31] F. Yu, W. Xian, Y. Chen, F. Liu, M. Liao, V. Madhavan, and T. Darrell, “Bdd100k: A diverse driving video database with scalable annotation tooling,” *arXiv preprint arXiv:1805.04687*, vol. 2, no. 5, p. 6, 2018.
- [32] P. Sun, H. Kretzschmar, X. Dotiwalla, A. Chouard, V. Patnaik, P. Tsui, J. Guo, Y. Zhou, Y. Chai, B. Caine, V. Vasudevan, W. Han, J. Ngiam, H. Zhao, A. Timofeev, S. Ettinger, M. Krivokon, A. Gao, A. Joshi, Y. Zhang, J. Shlens, Z. Chen, and D. Anguelov, “Scalability in perception for autonomous driving: Waymo open dataset,” in *Proceedings of the IEEE/CVF Conference on Computer Vision and Pattern Recognition (CVPR)*, June 2020.
- [33] T.-Y. Lin, P. Goyal, R. Girshick, K. He, and P. Dollár, “Focal loss for dense object detection,” in *Proceedings of the IEEE international conference on computer vision*, 2017, pp. 2980–2988.

- [34] T.-Y. Lin, M. Maire, S. Belongie, J. Hays, P. Perona, D. Ramanan, P. Dollár, and C. L. Zitnick, “Microsoft coco: Common objects in context,” in *European conference on computer vision*. Springer, 2014, pp. 740–755.
- [35] K. He, X. Zhang, S. Ren, and J. Sun, “Deep residual learning for image recognition,” in *Proceedings of the IEEE conference on computer vision and pattern recognition*, 2016, pp. 770–778.
- [36] W. Cao, V. Mirjalili, and S. Raschka, “Rank-consistent ordinal regression for neural networks,” *arXiv preprint arXiv:1901.07884*, 2019.
- [37] D. P. Kingma and J. Ba, “Adam: A method for stochastic optimization,” *arXiv preprint arXiv:1412.6980*, 2014.
- [38] K. Dembczyński, W. Kotłowski, and R. Słowiński, “Ordinal classification with decision rules,” in *International Workshop on Mining Complex Data*. Springer, 2007, pp. 169–181.